

Coherent control of low loss surface polaritons

Ali Kamli,^{1,2,3,*} Sergey A. Moiseev,^{1,4,†} and Barry C. Sanders¹

¹*Institute for Quantum Information Science, University of Calgary, Calgary, Alberta, Canada T2N 1N4*

²*Department of Physics, King Khalid University, Abha 61314, P O Box 9003, Saudi Arabia*

³*The National Centre for Mathematics and Physics, KACST, Riyadh, Saudi Arabia*

⁴*Kazan Physical-Technical Institute of the Russian Academy of Sciences, 10/7 Sibirsky Trakt, Kazan, 420029, Russia*

(Dated: December 10, 2018)

We propose fast all-optical control of surface polaritons (SPs) by placing an electromagnetically induced transparency (EIT) medium at an interface between two materials. EIT provides longitudinal compression and a slow group velocity while matching properties of the two materials at the interface provides strong transverse confinement. In particular we show that an EIT medium near the interface between a dielectric and a negative-index metamaterial can establish tight longitudinal and transverse confinement plus extreme slowing of SPs, in both transverse electric and transverse magnetic polarizations, while simultaneously avoiding losses.

PACS numbers: 42.50.Gy, 42.25.Bs, 78.20.Ci

Introduction:— All-optical rapid guidance, processing, and control of light in nanophotonic and quantum information applications is important but limited by weak nonlinearities in typical materials, the fast speed of light, and physical limitations to confinement such as enhanced absorption and the narrow spectral width of light. Strategies to overcome these speed and confinement weaknesses include exploiting photonic crystals with defect structures to trap light [1], surface polaritons (SPs) to confine light to wavelength dimensions [2] and use nonlinear interactions [3, 4], and electromagnetically induced transparency (EIT) to slow and compress light in the longitudinal propagation direction [5], which are realized in solid state [6], Bose-Einstein condensates [7], and Mott insulators [8]. We propose placing an EIT medium at the interface of two materials. This arrangement benefits from the combination of transverse confinement of surface polaritons with the longitudinal compression and slowing of pulses due to EIT.

We derive an analytical solution to the problem, which provides an elegant picture of EIT at a material interface, including hitherto unsuspected properties for the interface between a dielectric and a negative-index metamaterial (NIMM) [9]: our two key results for the dielectric-NIMM interface are (i) that this interface simultaneously supports both transverse electric (TE) and transverse magnetic (TM) polarizations whereas dielectric-dielectric and dielectric-metal interfaces only supports TM, and (ii) SP loss can be made arbitrarily small for the dielectric-NIMM interface but not for the other cases. Our analysis applies to general interfaces, but the dielectric-NIMM interface is especially intriguing and suggests possibilities of low-loss, fast control of both TM and TE polarized SPs.

For our scheme in Fig. 1, we suggest end-fire coupling excitation, which has been demonstrated experimentally with a high efficiency of 0.7 [10]. Our approach is to create two SP fields by directing two laser beams at the in-

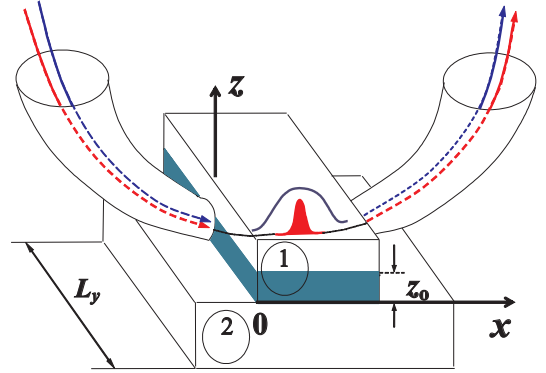


FIG. 1: (Color online) End-fire coupling scheme for coherent control of surface polaritons (SPs). Two incoming beams from the left waveguide create two SP pulses above the interface between media 1 and 2 in half-spaces $z > 0$ and $z < 0$, respectively: control (blue line) and signal probe (red filled). The SPs interact with a collection of Λ medium shown above the interface as a shaded green layer of thickness z_0 .

terface between two materials with permittivities ϵ_i and permeabilities μ_i (top: $i = 1$; bottom: $i = 2$), and these two SP fields propagate toward the EIT medium comprising three-level Λ atoms (3LA), quantum dots, nitrogen-valence centers in diamond, rare-earth ions in crystals, or similar (henceforth the ‘ Λ medium’); the three levels are designated $|\ell\rangle$ for $\ell \in \{1, 2, 3\}$, and the transition frequency $\omega_{\ell\ell'}$ corresponds to $|\ell\rangle \leftrightarrow |\ell'\rangle$. Our analysis does not restrict the signs of ϵ and μ hence accommodates dielectrics, surface plasmons at a dielectric-metal interface, and also NIMMs where both $\epsilon, \mu < 0$.

Absorption and dispersion of SP fields:— The SP fields, which propagate in the positive x -direction, are characterized by the ω -dependent complex wave vector $k_{\parallel} + i\kappa$. For $k_{\parallel}^2 = k_{\parallel}^2 - \omega^2 \epsilon_j \mu_j / c^2$, the wave vector com-

ponent normal to the interface, $k_1\varsigma_2 = -k_2\varsigma_1$ where $\varsigma \equiv \mu$ for the TE mode and $\varsigma \equiv \varepsilon$ for the TM mode; both polarizations coexist only if both conditions are simultaneously satisfied.

We analyze the SP modes at the interface between a dielectric and a NIMM media. Although the dielectric-NIMM interface is technically challenging, rapid progress is bringing metamaterials to the optical domain [11] thereby opening possibilities for optical storage and control [12]. The dielectric-NIMM interface is especially attractive because both TE and TM polarization modes can co-exist and, as we show below, complete suppression of SP losses is possible in principle thereby admitting novel opportunities in SP field control. Optical properties of the NIMM can be modeled with complex dielectric permittivity and magnetic permeability given by [9, 10]:

$$\varsigma_2(\omega) = \varsigma_r + i\varsigma_i = 1 - \frac{\omega_f^2}{\omega(\omega + i\gamma_f)} \quad (1)$$

for the two cases $\varsigma \equiv \varepsilon$, $f \equiv e$ and $\varsigma \equiv \mu$, $f \equiv m$. Here $\omega_{e,m}$ are the electric and magnetic plasma frequencies of the NIMM and $\gamma_{e,m}$ the loss rates, respectively. Accounting for complex ε and μ in the surface boundary conditions of SP wave vectors, we find (TM case)

$$k_{\parallel}(\omega) + i\kappa(\omega) = \frac{\omega}{c} \sqrt{\varepsilon_1\varepsilon_2(\varepsilon_2\mu_1 - \varepsilon_1\mu_2)/(\varepsilon_2^2 - \varepsilon_1^2)}, \quad (2)$$

and the TE case is similar. The real (imaginary) part of Eq. (2) yields SP TM mode dispersion (loss).

We study the system numerically at room temperature and at optical frequencies to determine its features. For metal, we use the values for Ag [13]: $\omega_e = 1.37 \times 10^{16} \text{s}^{-1}$, $\gamma_e = 2.73 \times 10^{13} \text{s}^{-1}$ and $\varepsilon_1 = 1.3$, $\mu_1 = 1$. As NIMM technology is embryonic, we consider a wide range of magnetic plasmon frequency such that $\omega_m \leq 0.5\omega_e$ [10], and γ_m is between $10^{-5}\gamma_e$ and γ_e itself.

Numerical results for $\kappa(\omega)$ are shown in Fig. 2 and reveal a deep abyss for all ω ; the abyss frequency ω_0 corresponds to a specific ratio of magnetic and electric loss for each ω , and Fig. 2 reveals $\kappa(\omega_0) \sim 0$, i.e. a complete cancelation of losses. From Eq. (2) ω_0 is determined with high accuracy from

$$\frac{\mu_i}{\varepsilon_i} = \frac{\mu_r(\varepsilon_r^2 + \varepsilon_1^2) - 2\varepsilon_r\varepsilon_1}{\varepsilon_r(\varepsilon_r^2 - \varepsilon_1^2)}, \quad (3)$$

which cannot be satisfied for an interface between a dielectric and metal because $\mu_1, \mu_2 > 0$. Figure 3 compares SP losses at a dielectric-NIMM interface for $\gamma_m = 10^{11} \text{s}^{-1}$ and $\omega_m = 0.5\omega_p$ and surface plasmon polaritons at a dielectric-metal interface.

We observe that NIMMs enable absorption losses to be drastically reduced in a narrow frequency band, as studied for freely propagating fields [14]. Here we predict a similar effect but for SP fields using a typical NIMM

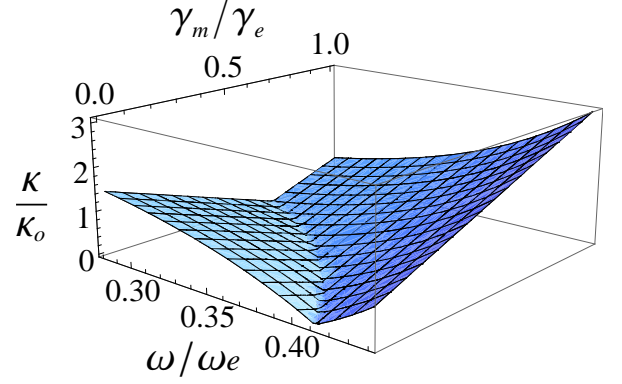


FIG. 2: (Color online) Absorption loss for surface polaritons as a function of frequency ω/ω_e and magnetic decoherence rate γ_m/γ_e , where $\kappa_0 = 10^4 \text{m}^{-1}$, $\gamma_e = 2.73 \times 10^{13} \text{s}^{-1}$, $\omega_m = 0.5\omega_e$ and $\varepsilon_1 = 1.3$, $\mu_1 = 1$.

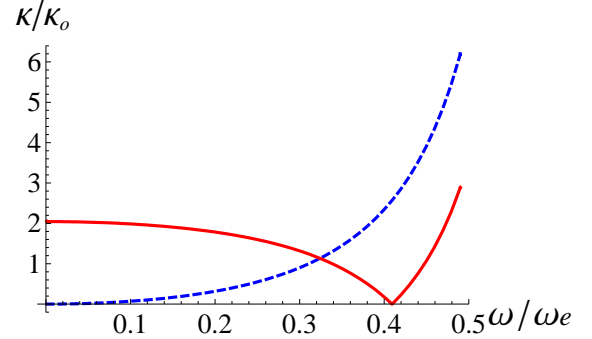


FIG. 3: (Color online) Comparison of SP losses at a dielectric-NIMM interface (red curve) and losses of surface plasmons at a dielectric-metal interface (blue curve) for $\gamma_m = 10^{11} \text{s}^{-1}$, $\gamma_e = 2.73 \times 10^{13} \text{s}^{-1}$ and $\omega_m = 0.5\omega_e$, $\omega_e = 1.37 \times 10^{16} \text{s}^{-1}$, $\omega_0 \cong 0.4092\omega_e$.

interface. Equation (3) shows that $\varepsilon_r, \mu_r < 0$ implies destructive interference between electric and magnetic absorption responses, which explains the high suppression of losses around ω_0 . The relative weakness of decay rates makes the frequency ω_0 sensitive to electric and magnetic decoherence rates as is evident from Fig. (2). Henceforth we demonstrate the possibility of coherent control of slow SP within frequency range around ω_0 of complete reduction of their losses in basic materials.

EIT control of SP modes:— Here we give a general analysis of EIT based coherent control of SP pulse interacting with a Λ medium near the surface. We assume that the probe field in the TM mode has a frequency ω_{31} and control field frequency equal to ω_{32} . The transition $|1\rangle \leftrightarrow |2\rangle$ is dipole-forbidden.

The SP electric field near the surface is obtained from field quantization [15] in a dispersive medium [16]. In the

plane wave expansion over modes indexed by λ ,

$$\hat{\mathbf{E}}(x, z) = \sum_{\lambda} \int dk_{\parallel} [\mathbf{E}_{0\lambda}(k_{\parallel}, z) \hat{a}_{\lambda}(k_{\parallel}) e^{ik_{\parallel}x} + \text{hc}], \quad (4)$$

with

$$[\hat{a}_{\lambda}(k_{\parallel}), \hat{a}_{\lambda'}^{\dagger}(k'_{\parallel})] = 2\pi\delta_{\lambda\lambda'}\delta(k_{\parallel} - k'_{\parallel}). \quad (5)$$

We develop the theory for TM; the TE case is then a straightforward generalization. Dropping λ , we obtain

$$\mathbf{E}_0(k_{\parallel}, z) = \begin{cases} (\mathbf{e}_x + \mathbf{i}e_z k_{\parallel}/k_1) E_0(k_{\parallel}) e^{-k_1 z}, & z > 0, \\ (\mathbf{e}_x - \mathbf{i}e_z k_{\parallel}/k_2) E_0(k_{\parallel}) e^{k_2 z}, & z < 0 \end{cases}. \quad (6)$$

Here $\mathbf{e}_x, \mathbf{e}_z$ are unit vectors along the \mathbf{x}, \mathbf{z} directions, with electric field amplitude

$$E_0(k_{\parallel}) = \sqrt{\hbar\omega(k_{\parallel})/2\pi\varepsilon_0 L_y L_z(\omega, \varepsilon, \mu)}, \quad (7)$$

and transverse quantization length $L_z = D + \frac{\omega^2(k_{\parallel})}{c^2} S$ with

$$D = \frac{\partial}{\partial\omega}(\omega\varepsilon_1) \frac{k_1^2 + k_{\parallel}^2}{k_1^3} + \frac{\partial}{\partial\omega}(\omega\varepsilon_2) \frac{k_2^2 + k_{\parallel}^2}{k_2^3},$$

$$S = \frac{\partial}{\partial\omega}(\omega\mu_1) \frac{\varepsilon_1^2}{k_1^3} + \frac{\partial}{\partial\omega}(\omega\mu_2) \frac{\varepsilon_2^2}{k_2^3}. \quad (8)$$

These quantities depend on the interface parameters and on the SP mode dispersion relation $\omega(k_{\parallel})$ of Eq. (2).

Adopting the usual EIT approximations [4, 17] for the evolution of a SP interacting with a Λ medium, we find the Fourier SP field equation

$$(\partial/\partial x - i\nu/v_0)\hat{A}(\nu, x) = -[\alpha(\nu) + \kappa(\omega_{31})]\hat{A}(\nu, x), \quad (9)$$

on the surface: $\hat{A}(\nu, x) = (2\pi)^{-1} \int dt e^{i\nu t} \hat{A}(t, x, z=0)$, where $\hat{A}(t, x, z=0) = \int dk_{\parallel} E_0(k_{\parallel}) \hat{a}(k_{\parallel}, t) e^{ik_{\parallel}x}$. By solving Eq. (9) we obtain the electric field over the surface

$$\hat{\mathbf{A}}(t, x, z > 0) = (\mathbf{e}_x + \mathbf{i}e_z k_{\parallel}(\omega_{31})/k_1^s) e^{-k_1^s z} \int d\nu e^{-i\nu t + [i\frac{\nu}{v_0} - \alpha(\nu) - \kappa(\omega_{31})]x} \hat{A}(\nu, 0) \quad (10)$$

where $\nu \equiv \omega(k_{\parallel}) - \omega_{31}$ is the SP field detuning from the central frequency ω_{31} , which is assumed to be close to ω_0 . Here $v_0 = \partial\omega/\partial k_{\parallel}$ is the SP group velocity without a 3LA Λ medium at $\omega = \omega_{31}$, and

$$\frac{\alpha(\nu)}{2\pi} = \frac{|g|^2}{v_0} \int_0^{\infty} \int_0^{L_y} dy dz \frac{n(\mathbf{r})(\gamma_{21} - i\nu)e^{-2k_1^s z}}{|\Omega_c(\mathbf{r})|^2 - (\nu + i\gamma_{21})(\nu + i\Gamma_{31})} \quad (11)$$

yields dispersion and absorption of the SP field, with Γ_{31} a linewidth, $\Omega_c(\mathbf{r})$ the control field Rabi frequency, $g = \mathbf{d} \cdot (\mathbf{e}_x + \mathbf{i}e_z k_{\parallel}/k_1) E_0(k_{\parallel}(\omega_{31})) / \hbar$ the SP- Λ coupling constant, \mathbf{d} the atomic dipole moment, and $n(\mathbf{r})$ the Λ

medium density. These parameters can be optimized for SP field control. Also the control field, which yields Ω_c , can be a freely propagating mode or a SP TE or TM field. Henceforth we assume $|\Omega_c(\mathbf{r})|^2 = |\Omega|^2 e^{-2k_1^c z}$, where k_1^s and k_1^c are the probe and control wave vectors in the z -direction for medium 1 as in Eq. (6).

Absorption and dispersion of the SP-field in the presence of a 3LA medium is given by $\alpha(\nu) + \kappa(\omega_{31})$ with inhomogeneous broadening at resonance transition $h = \Delta_w/\pi(\Delta^2 + \Delta_w^2)$ and inhomogeneous broadening width Δ_w . Thus $\Gamma_{31} = \Delta_w + \gamma_{31}$ where we have assumed that all atoms share the same decay constants γ_{mn} ; this assumption is reasonable for solid-state systems at liquid He temperatures because γ_{31}/Δ_w is negligible [4]. From Eq. (11), it follows that the field amplitude effectively is bounded by $z \leq \min\{1/k_1^s, 1/k_1^c\}$, and we assume confinement of the Λ medium to this height above the interface.

Eq. (11) is integrable for constant density $n(\mathbf{r}) \equiv n(0 < z < z_0) = n$, yields

$$\alpha(\nu, z_0) = \alpha_0(\omega_{31}) G(k_1^s, k_1^c, z_0, \beta(\nu)) \quad (12)$$

with

$$G(k_1^s, k_1^c, z_0, \beta) = \frac{i\Gamma_{31}}{\nu + i\Gamma_{31}} \left[{}_2F_1\left(1, \frac{k_1^s}{k_1^c}, \frac{k_1^s + k_1^c}{k_1^c}, \frac{1}{\beta(\nu)}\right) - e^{-2k_1^s z_0} {}_2F_1\left(1, \frac{k_1^s}{k_1^c}, \frac{k_1^s + k_1^c}{k_1^c}, \frac{e^{-2k_1^c z_0}}{\beta(\nu)}\right) \right] \quad (13)$$

a spectral function, ${}_2F_1$ the hypergeometric function, and $\beta \equiv (\nu + i\gamma_{21})(\nu + i\Gamma_{31})/|\Omega|^2$. Function (13) is a maximum $G = 1$ for $\nu = 0$ and depends on $\Delta_w, k_1^s/k_1^c, z_0$, and Ω_c , which provides rich opportunities for spectral and spatial control of the SP field.

As the formula is integrable, the resonant absorption coefficient for the Λ medium at ω_{31} is expressed in a simple form if the control field is off and $z_0 \gg 1/k_1^s$:

$$\alpha_0(\omega_{31}) = \pi n L_y |g|^2 / k_1^s v_0(\omega_{31}) \Gamma_{31} \quad (14)$$

with coupling constant $|g|^2 \sim 1/L_z$. An appropriate choice of materials can lead to small L_z hence considerably enhance the SP field amplitude and increase interaction coupling between the SP field and the 3LA Λ medium.

Numerical example:— Using our solution we demonstrate the exciting possibility of EIT control for the *low loss SP modes*, which opens opportunities to exploit spatial confinement and temporal control of SPs via their interaction with the Λ medium.

For $L_y = 2.5\mu\text{m}$, $0.4087\omega_e < \omega_{31} < 0.4097\omega_e$, we find $\kappa(\omega_{31}) < 0.01\kappa_0$, $v_0(\omega_{31}) \approx 0.6c$, $k_1^s(\omega_{31}) \approx 1\mu\text{m}^{-1}$. From Eqs. (7) and (14) for resonant optical transitions of rare earth ions in crystals, e.g. Pr³⁺-doped Y₂SiO₅ (demonstrated for EIT experiments [6]) with density $n \approx 10^{24}\text{m}^{-3}$, $\Gamma_{31} \approx 10^9\text{rad/s}$, $\gamma_{21}^{-1} \gg 1\mu\text{s}$, $\varepsilon_1 \approx 1.3$,

and $|\mathbf{d}| \approx -ea_0$ (with e the electron charge and a_0 the Bohr radius), we find $\alpha_0(\omega_{31}) \approx 10\mu\text{m}^{-1}$. Using Eq. (10) we compute time delay and group velocity for a Gaussian amplitude envelope of the SP probe input pulse $\exp[-(t/\delta t)^2/2]$ in the medium at $x = 0$.

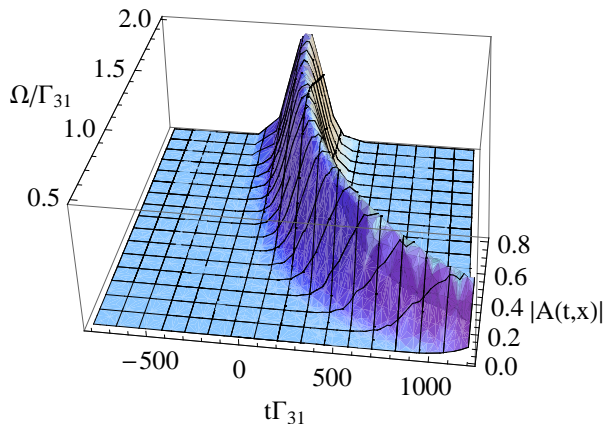


FIG. 4: (Color online) 3D graph of pulse propagation profile as a function of time $t\Gamma_{31}$ and control field amplitude Ω/Γ_{31} , $\Gamma_{31} = 10^9 \text{ rad/s}$, $\kappa(\omega_{31}) = 0.01\kappa_0 = 0.1 \times 10^3 \text{ m}^{-1}$.

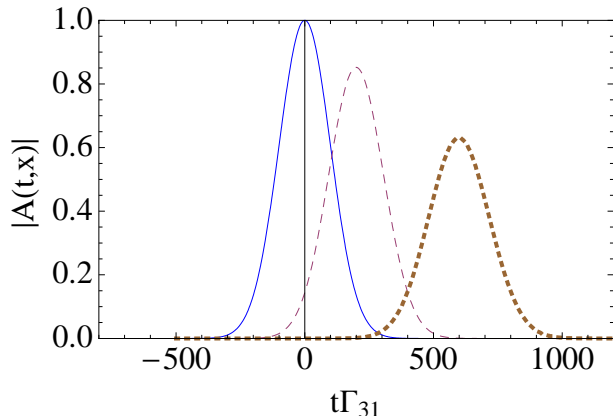


FIG. 5: (Color online) The pulse propagation profile as a function of time, $t\Gamma_{31}$, at different locations near the interface: blue (solid) at $x = 0$, red (dashed) at $x_1 = 1\text{mm}$, and brown (dotted) at $x_2 = 3\text{mm}$.

Input and output pulse profiles are presented in Figs. 4, 5 for input pulse duration $\delta t = 100\text{ns}$, for media lengths $x_1 = 1\text{mm}$ and $x_2 = 3\text{mm}$ ($< L = 1/\kappa$). As seen in Fig. 4 the time delay decreases with the control field amplitude as Ω^{-2} . Fig. 5 shows the pulse profile for $\Omega = \Gamma_{31}$ when it propagates a distance $x_1 = 1\text{mm}$ and $x_2 = 3\text{mm}$. The time delays are $t_{\text{delay}} = 2\delta t, 6\delta t$ respectively, whereas the amplitude has decreased only by factors 0.85 and 0.65, respectively. Thus the propagation length increased by more than $500/\alpha_0(\omega_{31})$ due to EIT of the SP field. Using these results we estimate the

group velocity $v_g \approx 5000\text{m/s}$ and a compressed longitudinal envelope of the SP pulse $l_{\text{SP}} = v_g \delta t = 0.5\text{mm}$, i.e. much smaller than the medium size. Thus the SP pulse can be successfully stored in the long-lived atomic coherence $\rho_{12}(t, x)$ and subsequently retrieved in accordance with an EIT quantum memory protocol [17].

Conclusion:— We have demonstrated low loss SPs at the interface between two media with quite general electromagnetic properties, including dielectrics, metals and metamaterials, and derived a closed form solution that provides deep insight into the system and control of spatially confined slow SP fields. We show that light pulses can be stored at the interface of two media exploiting EIT and low loss SP fields near a NIMM-dielectric interface.

We gratefully acknowledge financial support from iCORE, NSERC, CIFAR, KACST (Saudi Arabia), and RFBR grant # 06-02-16822.

* Electronic address: akamli@qis.ucalgary.ca

† Electronic address: smoiseev@qis.ucalgary.ca

- [1] S. G. Johnson and J. D. Joannopoulos, *Photonic Crystals: The Road from Theory to Practice* (Kluwer, Dordrecht, 2002).
- [2] V. M. Agranovich and D. L. Mills, *Surface Polaritons* (North Holland, Amsterdam, 1982).
- [3] K. J. Boller, A. Imamoglu, and S. E. Harris, Phys. Rev. Lett. **66**, 2593 (1991); J. E. Field, K. H. Hahn, and S. E. Harris, Phys. Rev. Lett. **67**, 3062 (1991); M. S. Bigelow, N. N. Lepeshkin, and R. W. Boyd, Phys. Rev. Lett. **90**, 113903 (2003); Science **301**, 200 (2003); R. W. Boyd and D. J. Gauthier, Prog. Opt. **XLIII**, ? (2002).
- [4] P. W. Milonni, *Fast Light, Slow Light and Left-Handed Light* (IOP, London, 2005).
- [5] L. V. Hau and S. E. Harris, Nature **297**, 594 (1999); Phys. Rev. Lett. **82**, 4611 (1999).
- [6] A. V. Turukhin et al, Phys. Rev. Lett. **88**, 023602 (2002).
- [7] C. Liu et al, Nature **409**, 490 (2001)
- [8] I. Carusotto et al, Phys. Rev. A **77**, 063621 (2008)
- [9] N. Engheta and R. W. Ziolkowski, *Metamaterials: Physics and Engineering Explorations* (Wiley, New Jersey, 2006).
- [10] S. A. Maier, *Plasmonics: Fundamentals and Applications* (Springer, New York, 2007).
- [11] U. K. Chettiar et al, Opt. Lett. **32**, 1671 (2007).
- [12] K. L. Tsakmakidis, A. D. Boardman and O. Hess, Nature (Lond.) **450**, 397 (2007); N. Papisimakis et al, arXiv:0801.1485 (2008).
- [13] M. A. Ordal et al, Appl. Opt. **24**, 4493 (1985).
- [14] J. Kastel, M. Fleischhauer, S. F. Yelin, and R. L. Walsworth Phys. Rev. Lett. **99**, 073602 (2007).
- [15] A. Kamli, and M. Babiker, Phys. Rev. A **62**, 043804 (2000).
- [16] L. D. Landau, E. M. Lifshitz, and L. P. Pitaevskii, *Electrodynamics of Continuous Media, 2nd ed.* (Elsevier, Oxford, 1984).
- [17] M. Fleischhauer, A. Imamoglu, and J. P. Marangos, Rev. Mod. Phys. **77**, 633 (2005).